ASTRONOMY
AND
ASTROPHYSICS

A new X-ray outburst in the globular cluster NGC 6440: SAX J1748.9-2021

J.J.M. in 't Zand[1], **F. Verbunt**[2], **T.E. Strohmayer**[3], **A. Bazzano**[4], **M. Cocchi**[4], **J. Heise**[1], **M.H. van Kerkwijk**[2], **J.M. Muller**[1,5], **L. Natalucci**[4], **M.J.S. Smith**[1,6], and **P. Ubertini**[4]

[1] Space Research Organization Netherlands, Sorbonnelaan 2, 3584 TA Utrecht, The Netherlands
[2] Astronomical Institute, P.O. Box 80000, 3508 TA Utrecht, The Netherlands
[3] NASA Goddard Space Flight Center, Code 666, Greenbelt, MD 20771, USA
[4] Istituto di Astrofisica Spaziale (CNR), Area Ricerca Roma Tor Vergata, Via del Fosso del Cavaliere, I-00133 Roma, Italy
[5] *BeppoSAX* Science Data Center, Nuova Telespazio, Via Corcolle 19, I-00131 Roma, Italy
[6] *BeppoSAX* Science Operation Center, Nuova Telespazio, Via Corcolle 19, I-00131 Roma, Italy

Abstract. For the second time in 27 years a bright transient X-ray source has been detected coincident with the globular cluster NGC 6440. It was found to be active in August, 1998, with the Wide Field Camera and the narrow field instruments on the *BeppoSAX* spacecraft, and with the All-Sky Monitor and the Proportional Counter Array on the *RossiXTE* spacecraft. Four X-ray bursts were detected, at least one of which shows the characteristics of a thermonuclear flash on a neutron star, in analogy with some ~ 20 optically identified low-mass X-ray binaries. The broad-band spectrum is hard as is common among low-mass X-ray binaries of lower luminosity ($\lesssim 10^{37}$ erg s^{-1}) and can be explained by a Comptonized model. During the burst the > 30 keV emission brightened, consistent with part of the burst emission being Compton up scattered within $\sim 10^{11}$ cm.

1. Introduction

If the ratio of the number of bright ($\gtrsim 10^{-9}$ erg cm^{-2}s^{-1} in 2 to 10 keV) X-ray sources to that of ordinary stars in Galactic globular clusters were the same as in the Galactic disk one would expect to find 0.1 bright X-ray source in all ~ 150 clusters combined. In reality, 12 are known. Comparison between these 12 sources and the bright X-ray sources in the Galactic disk sets the two populations further apart: for instance, $\sim 85\%$ of the globular cluster sources are X-ray bursters against only $\sim 20\%$ in the disk, none of the transient X-ray sources in globular clusters is a strong black hole candidate, many are in the disk.

Send offprint requests to: J.J.M. in 't Zand (jeanz@sron.nl)

These facts point to different evolutionary scenarios between both populations. The different average ages of both populations can only partly explain the different characteristics.

A few of the 12 bright X-ray sources in globular clusters are transient, implying they are only occasionally bright. One of these was detected in December 1971 in NGC 6440 (Markert et al. 1975). NGC 6440 is located close to the Galactic center, at a distance of 8.5 ± 0.4 kpc from us and 0.6 kpc above the Galactic plane (Martins et al. 1980, Ortolani et al. 1994). The distance is based on V and I photometry of horizontal branch stars in the color-magnitude diagram (Ortolani et al. 1994). The distance scale to globular clusters is currently being revised (e.g., Chaboyer et al. 1998); we will adhere to the distance of 8.5 kpc in this paper. NGC 6440 is fairly dense and apparently its core has not undergone a collapse, the core radius is $7.6''$ and the tidal radius $6.3'$ (Trager et al. 1993). Apart from the 1971 transient, one faint X-ray source was identified with ROSAT in NGC 6440 by Johnston et al. (1995). This source may or may not be related to the transient.

In this paper a new X-ray outburst in NGC 6440 is discussed. It was discovered with the Wide Field Cameras (WFC) on the *BeppoSAX* spacecraft in August 1998 (In 't Zand et al. 1998a), almost 27 years after the previous one was noticed. The All-Sky Monitor (ASM) on the *RossiXTE* spacecraft also made a weak detection. Follow-up observations were performed with the narrow-field instruments (NFI) on *BeppoSAX* and with the Proportional Counter Array (PCA) on *RossiXTE*. We present the analysis of the observations with these four sets of instruments and speculate on the nature of the source. The analysis of each data set concentrates on its specific qualities. In Sect. 2, we outline the discovery observations with WFC and study the long term behavior with WFC and ASM. In Sect. 3, we discuss the broad-band spectrum of the persistent emission as well as a burst detected with the NFI. The PCA observation is discussed in Sect. 4, it focuses on the short-term variability of the source. We review the results and their implications in Sect. 5.
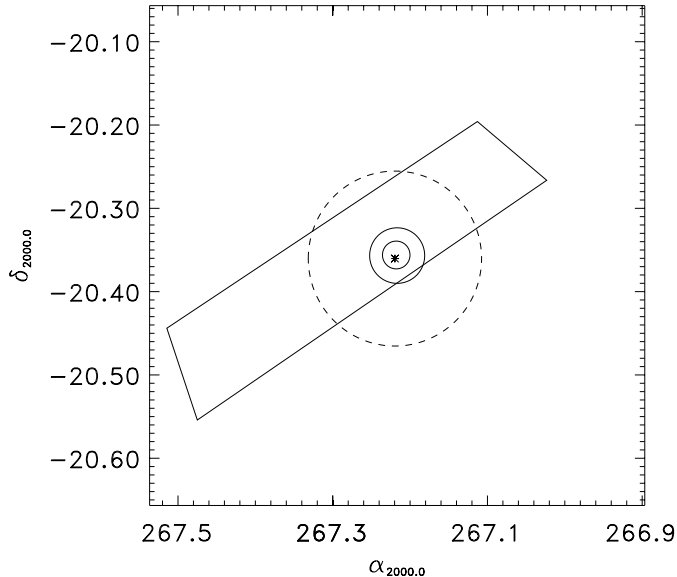
Fig. 1. The large solid circle is the 99% confidence error box from the WFC observation (In 't Zand et al. 1998a), the small solid circle that from the MECS observation. The quadrilateral is the combined Uhuru-OSO-7 error box for MX 1746-20 (Forman et al. 1976). The asterisk indicates the center of NGC 6440 (Picard & Johnston 1995), it has a core radius of $0°002$, the large dashed circle refers to the tidal radius. The coordinates are in degrees for equinox 2000.0

Table 1. Positions of NGC 6440 and coincident X-ray sources (Equinox 2000.0). ϵ is the uncertainty of the position quoted (better than 95% confidence)

Source[*]	R.A.	Decl.	ϵ
NGC 6440 center[a]	17h 48m 52.7s	$-20° 21'36.9''$	
MX 1746-200[b]	$267°11$	$-20°20$	
quadrilateral	$267°02$	$-20°27$	
coordinates	$267°47$	$-20°55$	
	$267°51$	$-20°44$	
SAX J1748.9-2021[c]	17h 48m 52s	$-20° 21'.4$	$2'$
SAX J1748.9-2021[d]	17h 48m 53.4s	$-20° 21'43''$	$1'$
ROSAT[e]	17h 48m 51.4s	$-20° 21'51''$	$5''$

[*]References: [a] Picard & Johnston 1995; [b] Forman et al. 1976; [c] In 't Zand et al. 1998a; [d] this publication; [e] Johnston et al. 1995

2. Discovery, bursts and long-term trend

The WFC (Jager et al. 1997) on the *BeppoSAX* satellite (Boella et al. 1997a) is carrying out a program of monitoring observations of the $40° \times 40°$ field around the Galactic center. The purpose is to detect X-ray transient activity, particularly from low-mass X-ray binaries (LMXBs) whose Galactic population exhibits a strong concentration in this field, and to monitor the behavior of persistently bright X-ray sources. Some previous results have been published in In 't Zand et al. (1998b), Heise (1998), Cocchi et al. (1998).

The program consists of campaigns during the spring and fall of each year. Each campaign lasts about two months and typically comprises weekly observations. Up to the spring 1998 campaign, a total net exposure time of 2 million seconds was accumulated during 4 campaigns. The fall 1998 campaign consists of five observations of ~ 50 ks each between August 22 and October 7, 1998.

During the first observation, on August 22.40–23.14, 1998, a transient was detected at a position consistent with that of the globular cluster NGC 6440 with a flux of ~ 30 mCrab (2–10 keV). The centroid position was $0'.3$ from the center of NGC 6440 (In 't Zand et al. 1998a, Picard & Johnston 1995). The source was designated SAX J1748.9-2021. The error box is indicated in Fig. 1 and specified in Table 1. The figure also includes the error box of the previous transient coincident with NGC 6440: MX 1746-20 which was detected with instruments on board the Uhuru and OSO-7 spacecrafts in December 1971 and January 1972 (Forman et al. 1976). ROSAT and optical observations of NGC 6440 were made soon after the WFC de-

tection and will be dealt with in a separate paper (Verbunt et al., in preparation).

The source was detected with WFC only during the August 22, 1998, observation. The last WFC observation prior to this was carried out on April 7, 1998 (137 days before the detection) with a 3σ upper limit of 5 mCrab (2–10 keV) at the position of SAX J1748.9-2021. The WFC observation following that of August 22 was performed on September 1, with an identical upper limit. These upper limits are about 6 times lower than the level during the detection. Given the rather sporadic coverage, we are unable to assess the duration of the transient activity from WFC data alone. Therefore, we studied data from the all-sky monitor (ASM) on *RossiXTE* (Levine et al. 1996)[1] which covers the period MJD 50094 through 51177 (Jan. 12, 1996, through Dec. 30, 1998). The ASM is less sensitive than the WFC per day of observation but this is compensated by a rather uniform and continuous coverage in time and sky position. At the position of NGC 6440, the 3σ detection limit in 1 day of exposure is about 30 mCrab in 2 to 10 keV but one should bear in mind that this can vary by roughly a factor 2 due to observational constraints.

In order to search for a significant ASM signal from a source in NGC 6440, we rebinned the data to a time resolution of 7 days. This increases the sensitivity to about 10 mCrab while preserving at least some information on the variability of the source and preventing that the transient signal smears out below the detection threshold. We varied the phasing of the binning in steps of 1 day to try to optimize the synchronization with the onset of the transient activity. A bias level was subtracted in the light curve to account for contributions from other non-transient sources (the region is likely to be source confused from time to time; GX 9+1 is only $3°$ from NGC 6440). This level was determined by weight averaging the data for periods at least 100 days from MJD 51047 (when it was detected with WFC). The result of this data reduction is that a source at NGC 6440 was detected above the ~ 10 mCrab detection threshold in one 7-day bin. The average intensity in this bin is 51 ± 8 mCrab. During

---

[1] the ASM measurements are publicly available at URL http://heasarc.gsfc.nasa.gov/docs/xte/asm_products.html
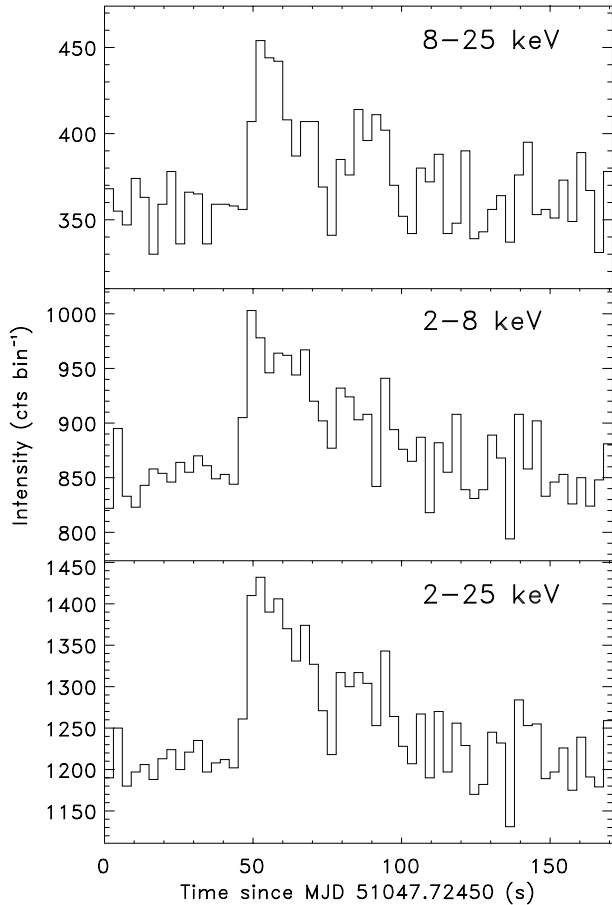
Fig. 2. Time profile of the second burst detected with WFC from SAX J1748.9-2021. Photons were accumulated over only that part of the detector illuminated by the source. No background was subtracted. The time resolution is 3 s

almost two years of coverage, NGC 6440 was brightest in this particular bin. The bin starts at MJD 51044. In the next 7-day bin the source is below a 3σ upper limit of 7 mCrab. Taking into account the last detection with NFI and PCA (Sects. 3 and 4, on MJD 51051) and the non-detection with WFC on MJD 51057, we conclude that SAX J1748.9-2021 was active at a level above 5 mCrab between 7 and 12 days.

Three bursts were detected with WFC, on MJD 51047.60976, 51047.72506 and 51047.84226. It is intriguing that the wait times differ by only 164 s or 1.7%. This reminds one of the narrow distribution of wait times found in GS1826-238 by Ubertini et al. (1999). A constant time interval between bursts in the case of SAX J1748.9-2021 would lead to three other bursts during the WFC observation, all of which coincide with Earth occultations or with standby mode of the instruments during passage of *BeppoSAX* through the South Atlantic Anomaly. Thus, we can neither confirm nor exclude a strict periodicity of burst times during our WFC observation. The bursts had peak intensities between 0.5 and 0.7 Crab units (2–10 keV). This is relatively faint for WFC and the time profiles (see Fig. 2) are rather noisy so that it is difficult to detect a softening of the spectrum during these bursts. The durations of the three bursts

were similar: about 100 s in the 2 to 10 keV band. The average spectrum of the three bursts, accumulated over 62 s of each burst (this covers both time intervals employed in Sect. 3.2), is consistent with a black body radiation model with a temperature of $kT = 2.31 \pm 0.18$ keV and a radius of $(4.9 \pm 0.8)d_{8.5 \text{ kpc}}$ km ($\chi_r^2 = 0.8$ for 69 dof; $d_{8.5 \text{ kpc}}$ is the distance in units of 8.5 kpc). Since a similar burst was detected with the more sensitive NFI as well (see Sect. 3), it was decided not to analyze the WFC-detected bursts any further.

The average spectrum of SAX J1748.9-2021 as measured with WFC is consistent with a power-law model with a photon index of 1.8 ± 0.2 and absorption by interstellar gas with cosmic abundances with a hydrogen column density of $N_H = (4.0 \pm 1.6) \times 10^{22}$ cm^{-2} (the cross section per hydrogen atom was taken from Morrison & McCammon 1983), the reduced χ^2 is $\chi_r^2 = 0.78$ for 21 dof (whenever an error for a spectral parameter is quoted throughout this paper, it refers to the single parameter 1σ error). The average flux was $(7.0 \pm 0.4) \times 10^{-10}$ erg cm^{-2}s^{-1} in 2 to 10 keV. Furthermore, the shape of the WFC-measured spectrum is also reasonably consistent with the Comptonized spectrum discussed in Sect. 3.1 (for the spectral parameters, see Table 2): $\chi_r^2 = 1.38$ for 23 dof. No variability was detected on time scales above 1 min, the 3σ upper limit on a time scale of 5 h was ~30%.

3. Broad-band spectral measurements with *BeppoSAX*-NFI

The NFI include 2 imaging instruments that are sensitive at photon energies below 10 keV: the Low-Energy and the Medium-Energy Concentrator Spectrometer (LECS and MECS, see Parmar et al. 1997 and Boella et al. 1997b respectively). They both have circular fields of view with diameters of 37 and 56 arcmin and effective bandpasses of 0.1–10 and 1.8–10 keV, respectively. The other two, non-imaging, NFI instruments are the Phoswich Detector System (PDS) which covers ~ 12 to 300 keV (Frontera et al. 1997) and the High-Pressure Gas Scintillation Proportional Counter (HP-GSPC) which covers 4 to 120 keV (Manzo et al. 1997).

A target-of-opportunity observation (TOO) was performed with the NFI four days after the WFC detection, on August 26.09–26.61 (i.e., 44.9 ks time span). The net exposure times are 10.0 ks for LECS, 23.0 ks for MECS, 12.0 ks for HP-GSPC and 22.2 ks for PDS. SAX J1748.9-2021 was strongly detected in all instruments and a ~100 s long X-ray burst was observed 32.9 ks after the start of the observation. The LECS and MECS images show only one bright source, the position as determined from the MECS image is consistent with that from WFC (Fig. 1 and Table 1). We applied extraction radii of 8′ and 4′ for photons from LECS and MECS images, encircling at least ~ 95% of the power of the instrumental point spread function, to obtain lightcurves and spectra. Long archival exposures on empty sky fields were used to define the background in the same extraction regions. These are standard data sets made available especially for the purpose of background determination. We note that the LECS and MECS backgrounds are not important for such a bright source as SAX J1748.9-2021. All spectra were rebinned
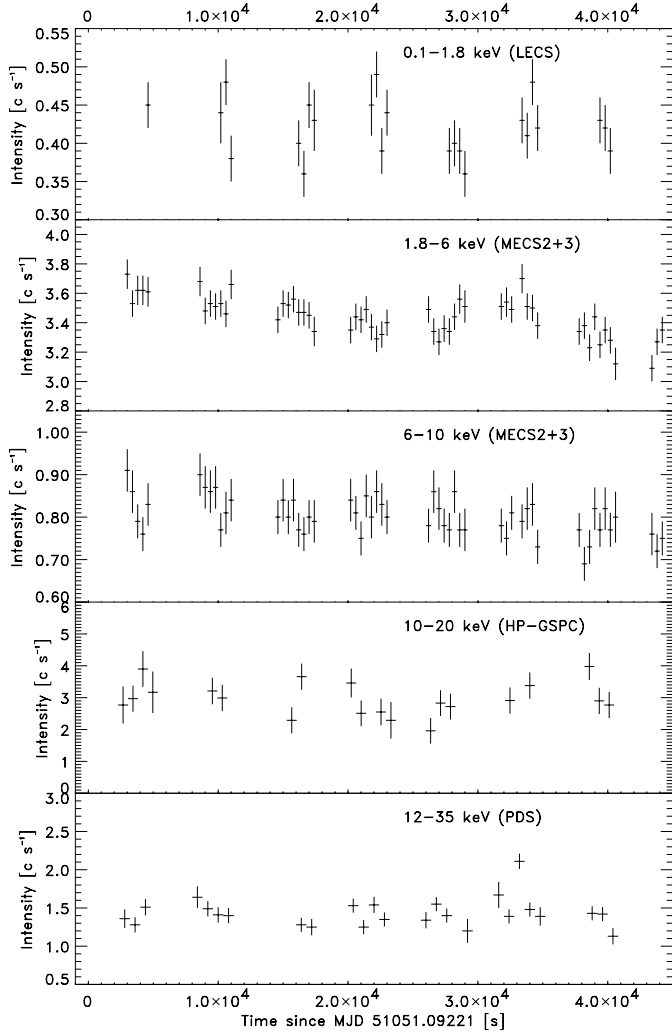
Fig. 3. Lightcurve as measured with the NFI in a number of bandpasses, corrected for background. The time resolutions are 400 s for the upper three panels and 800 s for the lower two panels. Data for the burst were excluded in these graphs. The background levels are from top to bottom 6.1×10^{-3}, 2.6×10^{-3}, 1.9×10^{-3}, 30 and 3 c s^{-1}

Table 2. Spectral parameters of four acceptable model fits to the persistent emission. Γ is the photon index. N_{H} is in units of 10^{22} cm^{-2}. The last line of each model specifies the χ^2_{r} values for the fit without a bb (black body) component (first 3 models) or with bb (last model). These values apply are after re-fitting the remaining parameters (or additional ones for the last model)

Model	broken power law + black body
N_{H}	0.86 ± 0.04
bb kT	0.97 ± 0.05 keV
Γ_{low}	1.54 ± 0.03
E_{break}	18.1 ± 1.2 keV
Γ_{high}	2.13 ± 0.04
χ^2_{r}	1.14 (190 dof)
χ^2_{r} without bb	1.27 (192 dof)
Model	high-energy cut off power law $(N(E)(:)E^{-\Gamma}$ for $E < E_{\mathrm{cutoff}}$ and $(:)E^{-\Gamma}\exp(-(E - E_{\mathrm{cutoff}})/E_{\mathrm{fold}})$ for $E > E_{\mathrm{cutoff}})$ + black body
N_{H}	0.82 ± 0.04
bb kT	0.90 ± 0.05 keV
Γ	1.44 ± 0.05
E_{cutoff}	2.3 ± 1.6 keV
E_{fold}	54.0 ± 5.2 keV
χ^2_{r}	1.01 (190 dof)
χ^2_{r} without bb	1.17 (192 dof)
Model	bremsstrahlung + black body
N_{H}	0.69 ± 0.02
bb kT	0.84 ± 0.02 keV
brems kT	46.6 ± 1.9 keV
χ^2_{r}	1.05 (192 dof)
χ^2_{r} without bb	3.55 (194 dof)
Model	Comptonized
N_{H}	0.32 ± 0.03
Wien kT_{W}	0.57 ± 0.01 keV
Plasma kT_{e}	15.5 ± 0.6 keV
Plasma optical depth τ	2.71 ± 0.08 for disk geometry 6.1 ± 0.2 for spherical geometry
Comptonization parameter y	0.9 for disk geometry 4.5 for spherical geometry
χ^2_{r}	1.07 (192 dof)
χ^2_{r} with bb	0.97 (190 dof)

so as to sample the spectral full-width at half-maximum resolution by three bins and to accumulate at least 20 photons per bin. The latter will ensure the applicability of χ^2 fitting procedures. A systematic error of 1% was added to each channel of the rebinned LECS and MECS spectra, to account for residual systematic uncertainties in the detector calibrations (e.g., Guainazzi et al. 1998). The bandpasses were limited to 0.1–4.0 keV (LECS), 2.2–10.5 keV (MECS), 4.0–25.0 keV (HP-GSPC) and 15–150 keV (PDS) to avoid photon energies where the spectral calibration of the instruments is not complete and where no flux was measured above the statistical noise. In spectral modeling, an allowance was made to leave free the relative normalization of the spectra from LECS, PDS and HP-GSPC to that of the MECS spectrum, to accommodate cross-calibration problems in this respect. Publicly available instrument response functions were used (version September 1997).

3.1. The persistent emission

Fig. 3 shows the lightcurve in various bandpasses. In the two MECS bandpasses a gradual intensity decline is visible by an amount of about 10%. The statistical quality of the LECS, HP-GSPC and PDS data does not allow a confirmation of this but these data do not contradict such a decline. On top of that, the lowest MECS bandpass shows a $\sim$ 5% hump between 27 and 40 ks into the observation (one might also interpret this as a dip before that). The X-ray burst occurred at 32.9 ks. Whether there is a physical correspondence between both is unclear. The
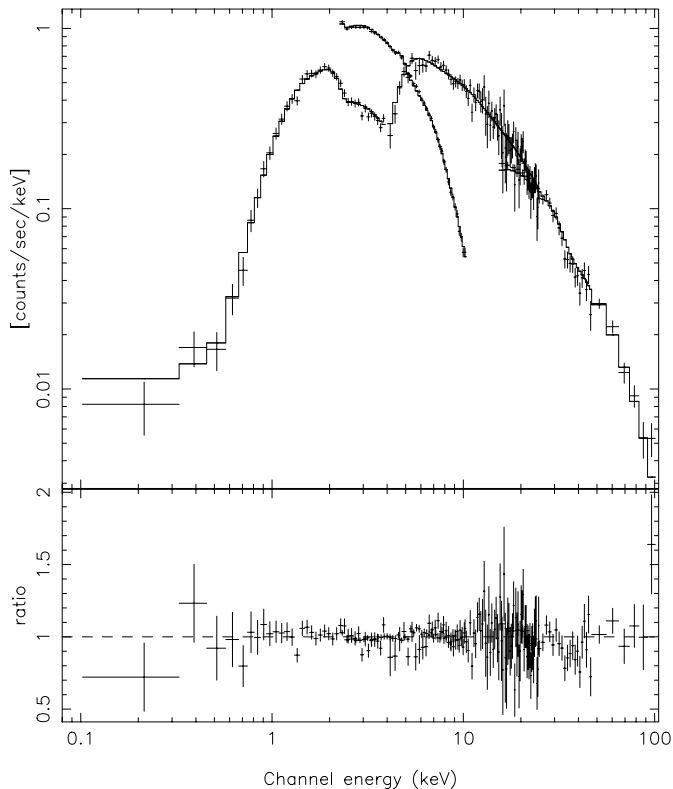
Fig. 4. *Upper panel:* count rate spectrum (crosses) and Comptonized spectrum model (histogram) up to 100 keV for average persistent emission. *Lower panel:* residual in units of count rate per channel.

statistical quality of the WFC data does not allow to check this for the three bursts that occurred during that observation.

A broad-band spectrum was accumulated, averaged over the complete observation, making use of the LECS, MECS, HP-GSPC, and PDS data. As stated above, the observation time intervals of the 4 instruments are not exactly overlapping. We tested for spectral variations using the MECS data and found no significant variation. This also applies to the 'hump'.

A simple absorbed power law function fits the data well between 1 and 40 keV and the parameter values are consistent with those found for the WFC data ($\chi_r^2 = 1.09$ for 172 dof, the photon index is $\Gamma = 1.72 \pm 0.01$ and $N_H = (1.17 \pm 0.03) \times 10^{22}$ cm^{-2}). However, such a model clearly fails when the complete bandpass is considered ($\chi_r^2 = 2.75$ for 196 dof). In order to explain the spectrum completely, one needs extra emission below 1 keV and a cut off above 40 keV. There are various ways by which this can be achieved with similar degrees of success. Four successful models are listed in Table 2. The Comptonized model is according to Titarchuk (1994)[2]. It is parametrized through the temperature T_W of the seed photons, the temperature T_e of the scattering electrons, and the optical depth of the electron cloud. Two of the four models are successful in describing 0.5–20 keV spectra of LMXBs in general: black body radiation plus either thermal bremsstrahlung or a Comptonized spectrum (e.g.,

---

[2] We used XSPEC as the tool to model spectra, in this tool the Comptonized model is identified as " comptt"

White et al. 1989, Christian & Swank 1997). This supports a LMXB classification of SAX J1748.9-2021.

In the bremsstrahlung model there is the necessity to include a black body component with a temperature equivalent of $kT = 0.84$ keV; the improvement in χ_r^2 is substantial. The other three models also improve when including a black body component but the improvement is marginal according to f-tests. A 1 keV black body feature has been detected in a number of other X-ray binary sources as well (e.g., Guainazzi et al. 1998, Oosterbroek et al. 1998, Kuulkers et al. 1997, Owens et al. 1997). In some cases it has been modeled by line emission instead of black body emission.

Independent of the model, the average 0.1–200.0 flux is $f_{bol} = 1.4 \times 10^{-9}$ erg cm^{-2}s^{-1} which implies, at a distance of 8.5 kpc, a luminosity of 1.2×10^{37} erg s^{-1} (or 3.4×10^{36} erg s^{-1} in 2–10 keV). The 2–10 keV flux is 44% lower than that measured with WFC four days earlier. The column density N_H is rather insensitive to the model for the continuum except when the Comptonized spectrum is considered. It lies between 0.32 and 0.86$\times 10^{22}$ cm^{-2}. This range is consistent with the value resulting from the interstellar reddening to NGC 6440: for $E_{B-V} = 1.00 \pm 0.10$ (Ortolani et al. 1994), $A_V = 3.10 \pm 0.31$ and $N_H = (1.79 \pm 0.1) \times 10^{21} A_V = (5.5 \pm 0.6) \times 10^{21}$ cm^{-2} (according to the conversion of A_V to N_H by Predehl & Schmitt 1995).

Christian & Swank (1997) successfully modeled the 0.5 to 20 keV spectra of 45 LMXBs by unsaturated Comptonization through a parametrization with a cutoff power law. A comparison of the parameter values for SAX J1748.9-2021 with those found by Christian & Swank shows that the power law index is normal for a burster. The value for E_{fold} is rather high. The values for the 8 bursters listed by Christian & Swank range between 5.3 and 25.0 keV. However, it should be noted that there is likely to be a selection effect in this parameter range because the upper boundary in the data is only 20 keV.

There are a few bursters which have been measured up to hundreds of keV (e.g., KS 1731-260, Barret et al. 1992; 4U 1728-34, Claret et al. 1994; Tavani & Barret 1997). With respect to these bursters, the high-energy spectrum of SAX J1748.9-2021 is not exceptionally hard. The sample of bursters with measured broad-band spectra is likely to grow in the near future; a number of NFI observations of bursters are currently being carried out by various investigators. Therefore, in due time, an unambiguous comparative analysis of all these spectra will be possible. In the mean time, the NFI study of the burster 1E 1724-308, located in the globular cluster Terzan 2 (Guainazzi et al. 1998) provides comparative material (see also, e.g., Barret et al. 1999). The NFI spectrum of 1E 1724-308 was successfully modeled through the Comptonization model by Titarchuk (1994) plus an additional soft component in the form of a ~ 1 keV black body radiator. The Comptonizing plasma has a temperature of ~ 30 keV and the seed photons have a temperature of 1 to 2 keV. Comparing the temperatures of the seed photons and the hot plasma, we note that these are about twice as cool in SAX J1748.9-2021 than in 1E 1724-308. Also, no additional soft component is needed in modeling the spec-
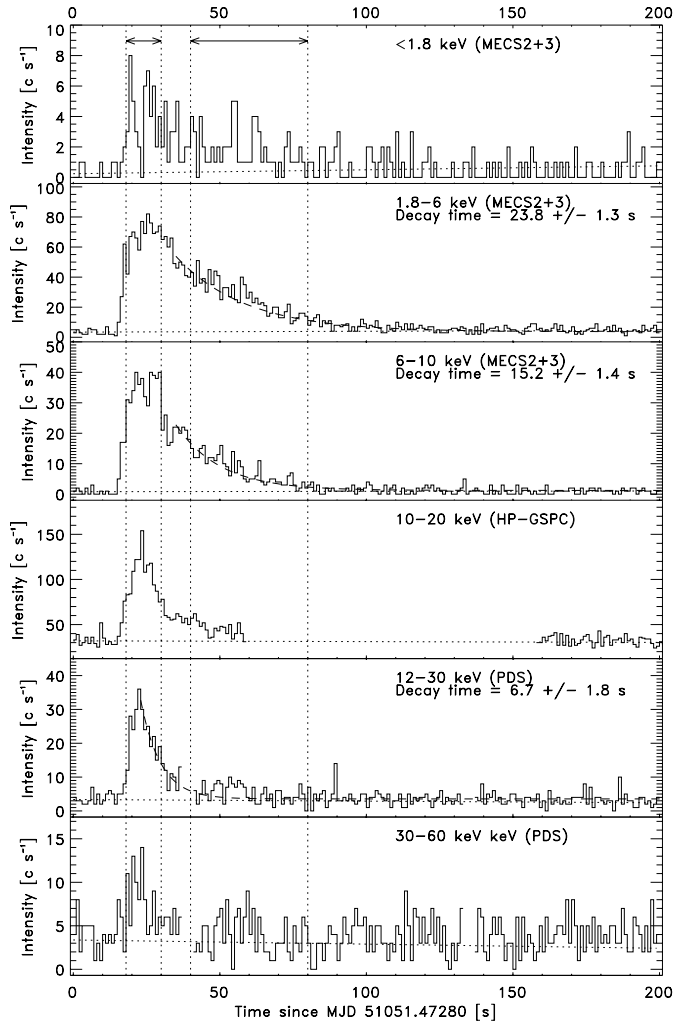
Fig. 5. Time profile of the burst detected from SAX J1748.9-2021 with MECS, HP-GSPC and PDS. The time resolution is 1 s. The curves have not been corrected for contributions from the background and the persistent emission. The linear trends as determined from the initial and final 10 s are drawn as near-horizontal dashed lines. The PDS curves were generated from collimator A and collimator B data, the gaps correspond to collimator slew times between off and on source position (these last 3 s and occur every 90 s). The HP-GSPC data only include those for when the collimator was in the on-source position. The vertical lines indicate the two time intervals for which spectra were modeled.

trum of SAX J1748.9-2021. We suggest that the differences between the two sources are due to a twice as low luminosity in SAX J1748.9-2021 which could be a reflection of a difference in accretion rate.

3.2. The burst emission

Fig. 5 shows the burst profile in a number of bandpasses from MECS, HP-GSPC and PDS data. There are no observations of the burst with the LECS. The 2 to 10 keV peak intensity is about 0.5 Crab units. This, as well as the duration, is similar to what was measured for the three bursts detected with WFC.
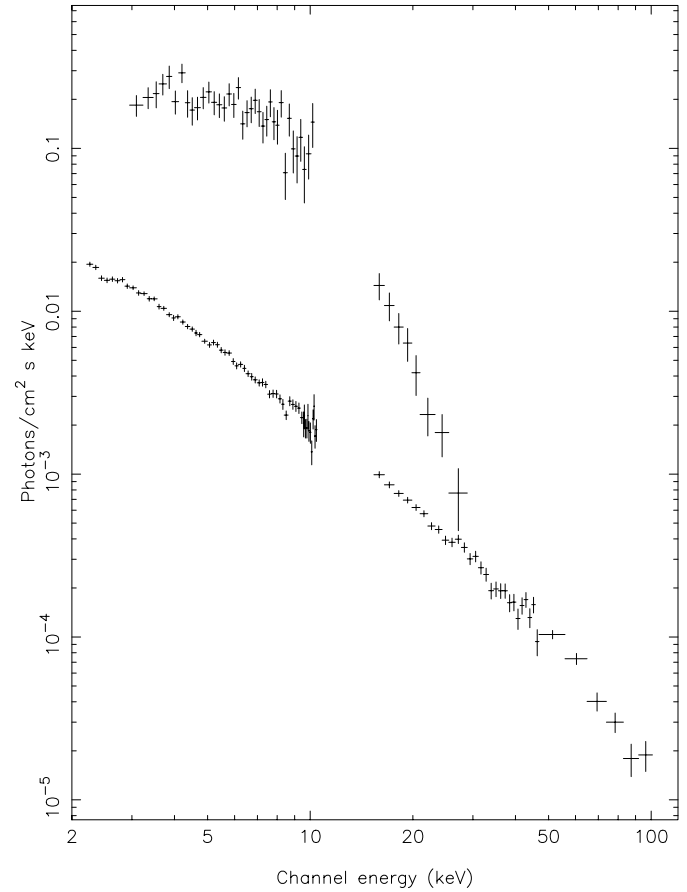

Fig. 6. Photon spectra for the first burst interval (18–30 s, upper spectrum) and for the persistent emission (lower spectrum), for MECS and PDS data only.

Table 3. Parameters of single spectral fit to burst and persistent data combined; $\chi_r^2 = 1.14$ (398 dof). The first burst interval encompasses MECS, HP-GSPC and PDS data, the second only MECS data

bb kT (keV)	2.25 ± 0.03 for 18–30 s interval
	1.67 ± 0.07 for 40–80 s interval
bb radius (km)	6.8 ± 0.2 for 18–30 s interval
for $d_{8.5 \text{ kpc}} = 1$	7.3 ± 0.9 for 40–80 s interval

The burst was divided in two time intervals (see Fig. 5) and spectra were generated from MECS (2.2–10.5 keV), HP-GSPC (4.0–15.0 keV) and PDS data (15.0–30.0 keV) for the first interval, and from MECS data (2.2–10.5 keV) for the second interval. The persistent emission was not subtracted in these spectra. We simultaneously modeled the spectra of these two intervals and of the persistent emission (from all 4 NFI) with the Comptonized model, whose parameters were fixed to the specification in Table 2, plus different black body models for the two burst time intervals. The results are given in Table 3 and Fig. 6 illustrates the spectrum.

The thermal nature of the burst spectrum with few keV temperatures and the cooling (Fig. 5, Table 3) are typical for a type I X-ray burst (e.g., Lewin et al. 1995). Such a burst is thought to

be due to a thermonuclear ignition of helium accumulated on the surface of a neutron star. The unabsorbed bolometric peak flux of the black body radiation is estimated at 1.7×10^{-8} erg cm^{-2}s^{-1}. For a distance of 8.5 kpc this translates into a peak luminosity of 1.5×10^{38} erg s^{-1}. This is near the Eddington luminosity for a 1.4 M$_\odot$ neutron star. We do not find evidence for photospheric expansion in this burst as the time profile shows no drops due to adiabatic expansion and the black body radius is consistent with a constant value over the two time intervals used for the spectral analysis. Therefore, we do not expect the luminosity to be much higher than the Eddington limit.

Currently, about 50 type I X-ray bursters are known (e.g., Van Paradijs 1995, Heise 1998). About 20 of these have optical counterparts and all of those are low-mass stars. The remaining bursters do not have optical counterparts because they are either situated in highly absorbed regions of the sky or are associated with transient X-ray sources whose position was not measured with sufficient accuracy. It is very likely that SAX J1748.9-2021 is a low-mass X-ray binary as well, especially since it appears associated with a globular cluster.

In the PDS, the photon count rate of the black body radiation is estimated to be negligible between 30 and 60 keV. For a $kT = 2.25$ keV black body model it is 4×10^{-3} times that in 12 to 30 keV. Nevertheless, the 30–60 keV PDS bandpass shows an increase during the first burst interval (Fig. 5). In this interval, the average of the increase in 30–60 keV photon count rate is 4.0 ± 0.5 c s^{-1} which compares to a level outside the burst interval of 1.01 ± 0.03 c s^{-1}. The ratio of the average 30–60 keV through 12–30 keV photon count rate increase during the first burst interval is 0.21 ± 0.03. We are unable to determine the > 30 keV spectrum during this interval due to insufficient statistics. If one assumes that the spectrum is the same as outside the burst, it implies that the level of Comptonization during the first burst interval increased by a factor of ~ 4. The close match between the < 30 and > 30 keV time profiles (Fig. 5) indicates that the presumed plasma is within $\sim 10^{11}$ cm of the neutron star surface which is the location of the black body radiation.

We note that the PDS data are crucial to observe the Comptonization of the burst emission. The MECS data by itself can satisfactorily be modeled by black body radiation only with N_H fixed at the value found from the persistent spectrum. For the first burst interval, $\chi_r^2 = 0.94$ for 35 dof and the temperature is slightly higher (2.37 keV).

No other bursts were observed during the NFI interval; this excludes that the time interval between bursts during the NFI observation is the same as that observed between the bursts during the WFC observation, in which case two more bursts should have been detected.

4. Rapid variability measurements with *RossiXTE*-PCA

A TOO was performed with *RossiXTE* on August 26.28–26.57, 4 days after the WFC detection. This TOO was nearly simultaneous to the one with NFI but the actual overlap with live NFI/MECS time is less than the exposure time, due to the different orbits of the two spacecrafts. The X-ray burst detected
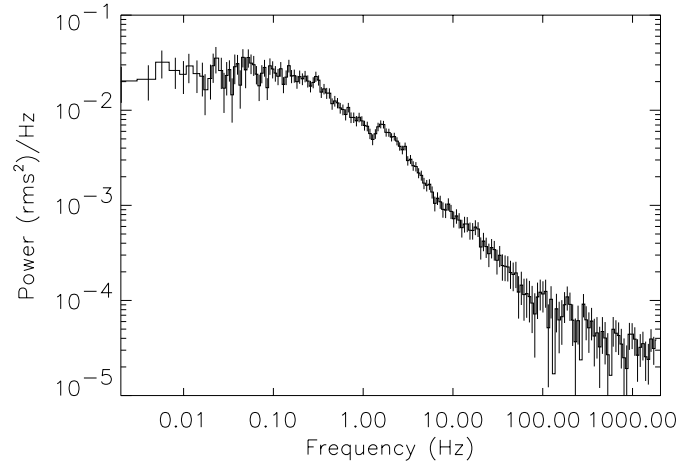

Fig. 7. Fourier power spectrum of the intensity time series as measured with *RossiXTE*-PCA between 2 and 20 keV

Table 4. Model parameters of broken power law fit to PCA Fourier power spectrum

Parameter	Value
Low-frequency index	0.058 ± 0.032
High-frequency index	0.940 ± 0.015
Break frequency	0.29 ± 0.02 Hz
rms (0.001 to 2048 Hz)	$4.8 \pm 0.3\%$
Bump start frequency	1.31 ± 0.06 Hz
Bump peak frequency	1.54 ± 0.07 Hz
Bump decay frequency	1.4 ± 0.1 Hz
rms (Bump start to 2048 Hz)	$6.8 \pm 0.8\%$

with the *BeppoSAX* NFI was missed by *RossiXTE* and no other bursts were detected with *RossiXTE*. The power spectrum of the 2 to 20 keV *RossiXTE* Proportional Counter Array (Zhang et al. 1993) time series shows no significant narrow features. The 90% confidence upper limit to any periodic signal power in the 100–900 Hz range is 0.37% (rms). The broad-band power spectrum computed from 9.7 ksec of data in the 2 to 20 keV range is shown in Fig. 7. It is typical of LMXBs of lower luminosity (i.e., with a luminosity at least one order of magnitude below the Eddington limit), being dominated by a power law above 0.2 Hz and flattening below. We fitted this spectrum with two components, a broken power-law and a "bump" between 1–2 Hz which we have modeled with a burst-like profile (linear rise, exponential decay). The derived power law indices, break frequency, location of the few Hz "bump", and the rms amplitudes of the components (see Table 4) are all consistent with broad-band power spectral measurements of other LMXB of lower luminosity (e.g., Wijnands & Van der Klis 1998a).

5. Discussion

The position, flux, spectrum and rapid variability are fully consistent with SAX J1748.9-2021 being the immediate neighborhood of a neutron star as part of a LMXB inside the Galactic globular cluster NGC 6440. The X-ray luminosity outside the

burst is $\sim 10^{37}$ erg s^{-1} which classifies the source as a LMXB of lower luminosity. This is consistent with the source being a type I burster and having a hard spectrum. It shows characteristics of an Atoll-type source (Hasinger & Van der Klis 1989, Van der Klis 1989).

The persistent spectrum can be well described by a number of models. In general, spectra of LMXBs of lower luminosity can be explained by a black body plus either thermal bremsstrahlung or a Comptonized spectrum. For SAX J1748.9-2021, both models fit the data equally well. Still, the most promising appears to be the Comptonized model whereby the spectrum is explained by soft photons that are Compton up scattered by a ~ 15 keV hot plasma. The reason that this model is preferred is because during a thermonuclear explosion on the neutron star the hard emission brightens simultaneously and dies out in the same fashion. The natural explanation of this is that photons created during the explosion are inverse-Compton scattered immediately by the hot plasma which is within $\sim 10^{11}$ cm of the neutron star. In case of thermal bremsstrahlung, the brightness would be linked to the mass accretion rate. In a thermonuclear flash it is not expected that the accretion rate increases and the thermal bremsstrahlung brightens.

Where is the source of the soft non-burst photons located? In order to obtain an expression for the equivalent spherical radius R_W of the emission area of the Wien spectrum, one needs to equalize the bolometric luminosity of the soft photons, L_{pers}, to that of a black body with temperature kT_W and radius R_W. L_{pers} can be obtained from integrating the observed spectrum (f_{bol}) and the distance d to the source. One will have to correct for energy gained by the photons in the inverse Compton scattering. The relative gain is given by the Comptonization parameter $y = 4kT_e\tau^2/m_ec^2$. R_W is then given by $R_W = 3 \times 10^4 d\sqrt{\frac{f_{bol}}{1+y}}/(kT_W)^2$ km where d is in kpc, f_{bol} in erg cm^{-2}s^{-1}, and kT_W in keV. If we apply the values of $f_{bol} = 1.4 \times 10^{-9}$ erg cm^{-2}s^{-1}, $y = 4.5$ (for spherical geometry) and $kT_W = 0.57$ keV, then $R_W \sim 13d_{8.5\ kpc}$ km. This implies that the soft photons are generated at the boundary layer between the accretion disk and the neutron star surface. The hot plasma is probably located to the outside of this layer because otherwise the spectrum would have been thermalized. The bolometric peak flux of the burst is 2.1×10^{-8} erg cm^{-2}s^{-1}, $\sim 20\%$ of this constitutes scattered photons.

The behavior of the Comptonized spectrum during the burst has been observed in one other LMXB before the launch of *BeppoSAX*: X1608–52 (Nakamura et al., 1989) with an instrument with a bandpass of 2 to 20 keV. The NFI on *BeppoSAX* in principle provide better means to test the Comptonization model on bursts because they combine to such a broad bandpass that the kT values for the Wien and plasma temperatures are within the bandpass. However, it is crucial that PDS data are available during the burst. Apart from the analysis presented here, we are aware of an NFI analysis of an X-ray burst in one other LMXB reaching similar conclusions: GS 1826-24 (Del Sordo et al. 1998).

On the basis of a short ROSAT HRI observation Johnston et al. (1995) report one dim ($L(0.5$–2.5 keV$) \simeq 1.2 \times 10^{33}$ erg s^{-1}) X-ray source near the core of NGC6440; a later longer observation indicates the presence of two sources (Verbunt 1998). At the moment it is not clear whether the transient corresponds to either of them; a ROSAT observation obtained on September 8, 1998, may shed light on this (Verbunt et al., in preparation). Considering the fact that no globular cluster contains two bright sources, we think it rather likely that SAX J1748.9-2021 is the same source as MX 1746-20 though this is not completely supported by the characteristics. The 2–10 keV spectrum of MX 1746-20 fits a power law with $\Gamma = 2.1^{+0.8}_{-0.5}$ and $N_H = (5.3^{+3.0}_{-2.0}) \times 10^{22}$ cm^{-2} (Markert et al. 1975). The photon index is compatible with the NFI spectrum of SAX J1748.9-2021 in that energy range but N_H is inconsistent. The peak flux of MX 1746-20 was about 150 mCrab, about five times brighter than the WFC detection of Aug 22, 1998. Such a variation of peak fluxes is not uncommon among recurrent transients (e.g., Chen et al. 1997, Levine 1998).

SAX J1748.9-2021 declined $44 \pm 5\%$ in 3.6 days. This is equivalent to an e-folding decay time of 6 ± 1 d. If the source declined exponentially, the intensity would have been 6 mCrab during the WFC observation on Sept. 1, equivalent with a 4σ signal. This is not inconsistent with the non-detection, as a 4σ signal after randomization might end up below a 3σ detection level. The $10\pm2\%$ drop in the 2–10 keV intensity during the NFI observation is equivalent to an e-folding decay time of 5 ± 1 d, in good agreement with the decay time above. For a decay time of 6 d and an activity onset 4 days before the WFC detection, as suggested by the ASM measurements, the peak flux would roughly be 57 mCrab. The 7-day average flux measurement with ASM is consistent with that.

Faint transient LMXBs that last only a few weeks are being discovered more and more, thanks to instruments on *BeppoSAX* and *RossiXTE* (Heise 1998, Remillard 1998). These short-period transients appear characterized by a peak luminosity well below the Eddington luminosity (by one to two orders of magnitude). SAX J1748.9-2021 belongs to this class of transients. The most appealing example of such a transient is SAX J1808.4–3658 (In 't Zand et al. 1998c) which revealed a pulsar signal and was determined to be in a tight binary system with a projected semi-major axis of only 1.9×10^9 cm (Chakrabarti & Morgan 1998, Wijnands & Van der Klis 1998b). One could speculate that the small outbursts of these transients are the consequence of a small accretion disk as fits in a short-period binary system. Confirmation of such speculation requires direct measurements of the orbital parameters of the binary.

Currently, bright (i.e., with an X-ray luminosity in excess of 10^{36} erg s^{-1}) X-ray sources are known in 12 Galactic globular clusters: in NGC 1851, 6440, 6441, 6624, 6652, 6712, 7078, Terzan 1, 2, 5, 6, and Liller 1. The sources in five of these are transient (e.g., Verbunt et al. 1995). The detection of X-ray bursts from SAX J1748.9-2021 leaves only one bright globular cluster source from which no X-ray bursts have been detected: Terzan 6 which contains one of the transients. The fraction of the number of type I X-ray bursters in low-mass X-ray bina-

ries in the Galactic disk is 30 to 40% (Van Paradijs 1995, Heise 1998), that in Galactic globular clusters is 92%. This difference was noted before and was partly suspected to be due to selection effects (infrequent and far-away bursters in the disk may easily go unnoticed). However, with the advent of WFC and its extensive program on the Galactic bulge, these selection effects have decreased considerably.

It has been suggested (e.g., In 't Zand et al. 1998b) that another difference between the LMXB populations in the disk and the globular clusters may be the fraction of transient systems which contain black hole candidates. For the disk it is at least 20% (Tanaka & Shibazaki 1996) and possibly as high as 70% (Chen et al. 1997). For a population of five LMXB transients in the clusters this percentage now is smaller than 20%. Assuming that 70% is the true value for both populations, the chance probability of finding no black hole candidate among the five cluster transients is 3%. Although intriguing, this number is not conclusive. Also, it is subject to uncertainty. For instance, as Deutsch et al. (1998) pointed out for NGC 6652, a classification as transient is only indisputable if a source varies by several orders of magnitudes (we note that similar classification problems exist for transients in the Galactic disk, e.g., Chen et al. 1997). The count of 5 transient LMXBs is based on a classification that flags a source as transient when it is usually below 10^{36} erg s^{-1} and occasionally brightens to above that threshold. This definition may include sources that vary less than orders of magnitude but happen to have an average luminosity close to the threshold. The source in NGC 6652 falls into that category. SAX J1748.9-2021 in NGC 6440 does not, it is four orders of magnitude above the quiescent level measured with ROSAT (Johnston et al. 1995). The only other indisputable transients are Terzan 6 and Liller 1. The chance probability of finding no black hole candidates among 3 transients is 12%.

References

Barret D., Bouchet L., Mandrou P., et al., 1992, ApJ 394, 615

Barret D., Grindlay J.E., Harrus I.M., Olive J.F., 1999, A&A 341, 789

Boella G., Butler R.C., Perola G.C., et al., 1997a, A&AS 122, 299

Boella G., Chiappetti L., Conti G., et al., 1997b, A&AS 122, 327

Chakrabarti D., Morgan E., 1998, Nat 394, 346

Chaboyer B., Demarque P., Kernan P.J., Kraus L.M., 1998, ApJ 494, 96

Chen W., Shrader C., Livio M., 1997, ApJ 491, 312

Christian D.M., Swank J., 1997, ApJS 109, 177

Claret A., Goldwurm A., Cordier B., et al., 1994, ApJ 423, 436

Cocchi M., Bazzano A., Natalucci L., et al., 1998, ApJ 508, L163

Del Sordo S., Frontera F., Pian E., et al., 1998, In: Bazzano A. (ed.) Proc. 3rd Integral Workshop: The Extreme Universe. Gordon & Breach, in press

Deutsch E.W., Margon B., Anderson S.F., 1998, AJ 116, 1301

Forman W., Jones C., Tananbaum H., 1976, ApJ 207, L25

Frontera F., Costa E., Dal Fiume D., et al., 1997, A&AS 122, 357

Guainazzi M., Parmar A.N., Segreto A., et al., 1998, A&A 339, 802

Hasinger G., Van der Klis M., 1989, A&A 225, 79

Heise J., 1998, In: Proc.: The Active X-ray Sky. Nucl. Ph. B 69, 186

In 't Zand J.J.M., Heise J., Bazzano A., et al., 1998a, IAU Circ. 6997

In 't Zand J.J.M., Verbunt F., Heise J., et al., 1998b, A&A 329, L37

In 't Zand J.J.M., Heise J., Muller J.M., et al., 1998c, A&A 331, L25

Jager R., Mels W.A., Brinkman A.C., et al., 1997, A&AS 125, 557

Johnston H.M., Verbunt F., Hasinger G., 1995, A&A 298, L21

Kuulkers E., Parmar A.N., Owens A., Oosterbroek T., Lammers U., 1997, A&A 323, L29

Levine A., 1998, In: Proc.: The Active X-ray Sky. Nucl. Ph. B 69, 196

Levine A., Bradt H., Cui W., et al., 1996, ApJ 469, L33

Lewin W.H.G., Van Paradijs J., Taam R.E., 1995, In: Lewin W.H.G., van Paradijs J.,van den Heuvel E.P.J. (eds.) X-ray Binaries. Cambridge University Press, Cambridge, p. 175

Manzo G., Giarusso S., Santangelo A., et al., 1997, A&AS 122, 341

Markert T.H., Backman D.E., Canizares C.R., Clark G.W., Levine A.M., 1975, Nat 257, 32

Martins D.H., Harvel C.A., Miller D.H., 1980, AJ 85, 521

Morrison R., McCammon D., 1983, ApJ 270, 119

Nakamura N., Dotani T., Inoue H., Mitsuda K., Tanaka Y., 1989, PASJ 41, 617

Oosterbroek T., Parmar A.N., Mereghetti S., Israel G.L., 1998, A&A 334, 925

Ortolani S., Barbuy B., Bica E., 1994, A&AS 108, 653

Owens A., Oosterbroek T., Parmar A.N., 1997, A&A 324, L9

van Paradijs J., 1995, In: Lewin W.H.G., van Paradijs J.,van den Heuvel E.P.J. (eds.) X-ray Binaries. Cambridge University Press, Cambridge, p. 536

Parmar A.N., Martins D.D.E., Bavdaz M., et al., 1997, A&AS 122, 309

Picard A., Johnston H.M., 1995, A&AS 112, 89

Predehl P., Schmitt J.H.M.M., 1995, A&A 293, 889

Remillard R., 1998, In: Giovanelli F., Sabau-Graziati L. (eds.) Proc.: Multifrequency Behavior of High Energy Cosmic Sources. Vulcano, May 1997, in press

Tanaka Y, Shibazaki N., 1996, ARA&A 34, 607

Tavani M., Barret D., 1997, In: Dermer C.D., Strickman M.S., Kurfess J.D. (eds.) Proccedings of the 4th Compton Symposium, AIP Conf. Proc. 410, 75

Titarchuk L., 1994, ApJ 434, 313

Trager S.C., Djorgovski S., King I.R., 1993, In: Djorgovski S.G., Meylan G. (eds.) Structure and Dynamics of Globular Clusters. ASP, San Francisco, p. 347

Ubertini P., Bazzano A., Cocchi M., et al., 1999, ApJL, in press

Van der Klis M., 1989, In: Hunt J., Battrick B. (eds.) Proc. 23rd ESLAB Symposium on: Two Topics in X-ray Astronomy. ESA SP-296, p. 203

Verbunt F., 1998, In: Aschenbach B., Freyberg M. (eds.) Highlights in X-ray astronomy. MPE Report, in press

Verbunt F., Bunk W., Hasinger G., Johnston H.M., 1995, A&A 300, 732

White N.E., Stella L., Parmar A.N., 1989, ApJ 324, 363

Wijnands R., van der Klis M., 1998a, submitted to ApJ (astro-ph/9810342)

Wijnands R., van der Klis M., 1998b, Nat 394, 344

Zhang W., Giles A.B., Jahoda K., et al., 1993, Proc. SPIE 2006, 324